Talanta 271 (2024) 125686

Contents lists available at ScienceDirect

Talanta

journal homepage: www.elsevier.com/locate/talanta

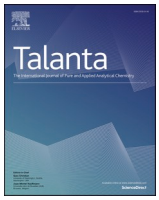

One-phase extraction coupled with photochemical reaction allows the in-depth lipid characterization of hempseeds by untargeted lipidomics

Andrea Cerrato [a], Sara Elsa Aita [a], Giuseppe Cannazza [b,c], Chiara Cavaliere [a], Alberto Cavazzini [d], Cinzia Citti [b,c], Carmela Maria Montone [a,*], Enrico Taglioni [a], Aldo Laganà [a]

[a] Department of Chemistry, Sapienza University of Rome, Piazzale Aldo Moro 5, 00185, Rome, Italy
[b] Department of Life Sciences, University of Modena and Reggio Emilia, Via Campi 103, Modena, 41125, Italy
[c] Institute of Nanotechnology – CNR NANOTEC, Campus Ecotekne, Via Monteroni, Lecce, 73100, Italy
[d] Department of Chemical, Pharmaceutical and Agricultural Sciences, University of Ferrara, Via L. Borsari 46, Ferrara, 44121, Italy

ARTICLE INFO

Keywords:
High-resolution mass spectrometry
Cannabis sativa
Aza-paternò-büchi
Double bond location
Fatty acids
Phospholipids

ABSTRACT

Due to their valuable nutritional content, several hemp-derived products from hempseeds have recently been placed in the market as food and food ingredients. In particular, the lipid composition of hempseeds has raised interest for their rich content in biologically active polyunsaturated fatty acids with an optimum ratio of omega-3 and omega-6 compounds. At present, however, the overall polar lipidome composition of hempseeds remains largely unknown. In the present work, an analytical platform was developed for the extraction, untargeted HRMS-based analysis, and detailed annotation of the lipid species. First, five one- and two-phase solid-liquid extraction protocols were tested and compared on a hempseed pool sample to select the method that allowed the overall highest efficiency as well as easy coupling with lipid derivatization by photochemical [2 + 2] cycloaddition with 6-azauracil. Underivatized lipids were annotated employing a data processing workflow on Compound Discoverer software that was specifically designed for polar lipidomics, whereas inspection of the MS/MS spectra of the derivatized lipids following the aza-Paternò-Büchi reaction allowed pinpointing the regiochemistry of carbon-carbon double bonds. A total of 184 lipids were annotated, i.e., 26 fatty acids and 158 phospholipids, including minor subclasses such as N-acylphosphatidylethanolamines. Once the platform was set up, the lipid extracts from nine hempseed samples from different hemp strains were characterized, with information on the regiochemistry of free and conjugated fatty acids. The overall analytical approach helped to fill a gap in the knowledge of the nutritional composition of hempseeds.

1. Introduction

Industrial hemp strains of cannabis sativa, which are characterized by low content in psychoactive Δ^9-tetrahydrocannabinol (Δ^9-THC), have been mainly employed as a source of sustainable and economic fibers in the textile industry [1]. The Council Directive 2002/53/EC enlists the industrial hemp varieties among the common catalog of the varieties of agricultural plant species that can be cultivated and marketed in the European Union [2]. Following the revitalization of the cultivation and supply chain of industrial hemp, several hemp-derived products from hempseeds have recently been placed in the market as food and food ingredients [3]. Despite being long treated as a byproduct of fiber production, hempseeds are nowadays considered a rich source of dietary proteins, lipids, fibers, vitamins, and minerals [4]. Hempseed-derived peptides have shown promising results for their health-promoting activities [5,6], highlighting the presence of short-chain peptides with significant hypotensive and cholesterol-lowering activity. Moreover, hempseeds and hempseed oil have gained attention for their high content of polyunsaturated fatty acids (PUFA) belonging to the omega-3 (ω-3) and omega-6 (ω-6) classes. These essential fatty acids (FA) cannot be synthesized by mammals and are converted to very long-chain PUFA (e.g., arachidonic acid, ω-6, and eicosapentaenoic acid, ω-3) [7]. Within the human body, ω-3 and ω-6 very-long-chain PUFA are well-known to exert primary albeit opposite functions, with the former responsible for anti-inflammatory and vasodilatory activities [8] and the latter capable of promoting inflammation and constriction of blood vessels [9]. As such, absolute content and proportions of the dietary intake of ω-3 and ω-6 PUFA play a significant

* Corresponding author.
E-mail address: carmelamaria.montone@uniroma1.it (C.M. Montone).

https://doi.org/10.1016/j.talanta.2024.125686
Received 27 November 2023; Received in revised form 10 January 2024; Accepted 15 January 2024
Available online 17 January 2024

role in regulating body homeostasis [10], and hempseeds are known to contain a unique and balanced FA composition, with a ratio ω-6/ω-3 around 3 [11]. The interest in vegetable sources of ω-3 and ω-6 PUFA as an alternative to fish and fish oils has risen given that vegetarians/vegans, non-fish eaters, and pregnant people may not consume adequate quantities of these compounds [12]. Having a nutrient profile similar to nuts, hempseeds contain FA in their free form or bound to other lipid structures, such as glycerolipids (GL) and glycerophospholipids (GP) [11]. To comprehensively characterize the lipidome of hempseeds and its derivatives, high-resolution mass spectrometry (HRMS)-based lipidomics represents the prime analytical approach. Buré et al. characterized the FA and GP content of hempseed cakes [13], whereas Kozub et al. explored the GL composition of hempseed cold-pressed oil [14]. Recently, Bakhytkyzy et al. [15] set up an analytical platform based on micro-solid phase extraction and HRMS for annotation and relative quantification of 65 lipids in hempseed oil. In HRMS-based lipidomics, one of the major current issues is the determination of the regiochemistry of FA, i.e., the geometry and position of carbon-carbon double bonds [16,17]. Over the years, several different approaches have been proposed for pinpointing carbon-carbon double bonds, including ozone-induced fragmentation [18], ultraviolet photodissociation [19], and Paternò–Büchi (PB) derivatization [20,21]. Among these, PB reactions have gained significant attention since they are independent of specific instrumentation or extensive sample preparation, allowing several applications in the clinical research field [22–24]. In foodomics and food analysis, few papers have dealt with the double bond location of FA in lipid structures. Liu et al. employed the PB reaction for pinpointing carbon-carbon double bonds in phospholipids of bovine milk [25], whereas Coniglio et al. annotated the double bond location of FA in arsenosugar phospholipids from seaweeds by epoxidation and HRMS [26]. In the present study, a deep and detailed untargeted lipidomics study was carried out on hempseed lipid extracts from 9 industrial hemp strains. After evaluating the optimum extraction workflow, an aza-Paternò–Büchi (aPB) derivatization reaction with 6-azauracil (6-AU) was employed before HRMS analysis and data processing. The aPB reaction was proven to be more effective than the common PB reaction when used in combination with higher collisional dissociation (HCD) and negative ion mode [27]. The overall analytical strategy led to filling a void in the knowledge of the composition of the polar lipidome of hempseeds and its variability in different strains.

2. Materials and methods

2.1. Lipid nomenclature

Shorthand notation of the lipid species was based on the guidelines of LIPID MAPS [28,29]. The location of carbon-carbon double bonds was based on the ω-nomenclature, in which the carbon atoms are counted from the terminal atom of the fatty acyl chain. Underscore ("_") indicates that the *sn*-position is unspecified.

2.2. Chemicals and materials

Optima mass spectrometry (MS) grade water, acetonitrile (ACN), methanol (MeOH), and isopropanol (iPrOH) were purchased from Thermo Fisher Scientific (Waltham, MA, United States). Glacial acetic acid, ammonium acetate, 6-AU, chloroform, and n-butanol (n-BuOH) were purchased from Merck (Darmstadt, Germany). A mixture of isotope-labeled lipids (Splash Lipidomix) containing phosphatidylcholine (PC) 15:0–18:1-d_7, phosphatidylethanolamine (PE) 15:0–18:1-d_7, phosphatidylserine (PS) 15:0–18:1-d_7, phosphatidylglycerol (PG) 15:0–18:1-d_7, phosphatidylinositol (PI) 15:0–18:1-d_7, phosphatidyl acid (PA) 15:0–18:1-d_7, at nominal concentrations of about 5–160 μg/mL as well as oleic acid-d_9 (internal standard, IS) were purchased from Merck. PTFE filters (0.20 m, 15 mm) were acquired from (Sartorius AG, Goettingen, Germany).

The hempseeds samples were provided by CREA-CI (Research Center for Cereal and Industrial Crops, Bologna, Italy). In particular, seeds from six *C. sativa* varieties, including Carmaleonte (chemotype III), Eletta Campana (chemotype III), FINOLA (chemotype III), Futura 75 (chemotype III), Santhica 27 (chemotype IV), USO 31 (chemotype V), and Ermo (chemotype V), and two accessions, including Felsinea (chemotype IV) and S435 (chemotype III), were selected for this work.

2.3. Choice of the extraction procedure

Dry hempseeds were pooled, ground, and homogenized before extraction. Comparative lipid extractions were carried out on 400 mg aliquots ($n = 3$) of pooled samples by five different methods. Protocol I consisted of a modified version of the extraction method outlined by Bligh and Dyer (B&D) [30]. Briefly, 400 mg of the pooled sample was added to 2.1 mL of MeOH and vortexed for 2 min at room temperature. Then, 2.1 mL of $CHCl_3$ was added, and the mixture was vortexed for 2 more min at room temperature. Finally, 1.8 mL of water was added into the glass tube and the mixture was kept vortexing for 20 min. Samples were centrifuged at 3000×*g* at 20 °C for 15 min allowing for phase separation. The lower layer was finally transferred to a new glass tube and evaporated with a Speed-Vac SC 250 Express (Thermo 164 Avant, Holbrook, NY, USA). Protocol II was a biphasic lipid extraction based on the procedure proposed by Matyash [31] using MTBE/MeOH/H_2O (10:3:2.5, *v/v/v*). MeOH (1.16 mL) was added to a 400 mg sample aliquot, which was placed into a glass tube, and then vortexed for 2 min. Then, 3.87 mL of MTBE was added, and the mixture was kept vortexing for 1 h at room temperature. Finally, phase separation was obtained by mixing 0.970 mL of water. After 10 min of incubation at room temperature, the sample was centrifuged at 3000×*g* for 15 min at 20 °C. The upper phase was collected and put into another glass tube and evaporated with a Speed-Vac SC 250 Express. Protocol III was conducted by mixing 400 mg of the pooled sample with 6 mL of *n*-BuOH/MeOH (3:1, *v/v*, BuMe), vortexed for 20 min, centrifuged at 3000×*g*, and evaporated [32]. Protocol IV consisted of a monophasic extraction using EtOH as solvent by mixing 400 mg of pooled samples with 6 mL of MeOH in a glass tube put under agitation for 30 min. Then, samples were centrifuged at 3000×*g* at 20 °C for 15 min and evaporated. Finally, protocol V consisted of a monophasic extraction using MeOH as the only extraction solvent. The extraction was performed essentially as described for EtOH. All extracts from protocols I–V were then resuspended in 6 mL of MeOH. Later 800 μL of each extract was mixed with 150 μL of water and 50 μL of $CHCl_3$ to reach the phase composition at MeOH/H_2O/$CHCl_3$ (80:15:5, v/v/v). Before UHPLC-HRMS analysis, 5 μL of IS solution was added to each sample, and all extracts were filtered through PTFE filters (0.20 μm, 15 mm). To evaluate the extraction procedures, 16 lipids were monitored: six fatty acids (FA 16:0, FA 18:3, FA 18:2, FA 18:1, FA 18:0, FA 20:1), two PA (PA 16:0_18:2 and PA 18:2/18:2), two PE (PE 16:0_18:2 and PE 18:2/18:2), two PG (PG 16:0_18:2 and PG 18:2/18:2), two PC (PC 16:0_18:2 and PC 18:2/18:2), and two PI (PI 16:0_18:2 and PI 18:2/18:2). Following the choice of the extraction procedure, three aliquots of each of the 9 hempseed samples were subjected to lipid extraction following protocol 5.

2.4. Offline aPB reaction

For the determination of carbon−carbon double bonds in fatty acyl chains, aPB reaction of lipids with 6-AU was conducted on the lipid extracts as previously reported with some modifications [27]. The reaction solution containing aPB reagent (6-AU, 24 mM) was prepared in MeOH. Then, 600 μL of each of the lipid extracts that were obtained through protocol 5 were added to 75 μL of MeOH, 125 μL of 6-AU solution, 50 μL of $CHCl_3$, and 150 μL of water. Subsequently, each sample solution was filtered through PTFE filters (0.20 μm, 15 mm) directly into a quartz cuvette, and purged with nitrogen gas to remove residual oxygen. The cuvette was irradiated at 254 nm using a Spectroline E-series

UV lamp with shortwave emission (Thermo Fisher Scientific) for 30 min at room temperature. Next, reaction mixtures were collected, and a 195 μL aliquot was put in a glass vial with 5 μL of IS mixture before UHPLC-HRMS. Three independent experiments were conducted for each sample.

2.5. UHPLC-HRMS analysis

Underivatized and derivatized lipid separation was carried out by a Vanquish binary pump H (Thermo Fisher Scientific, Bremen, Germany), equipped with a thermostated autosampler and column compartment, on a C8 Hypersyl GOLD (100 × 2.1 mm, 1.9 μm particle size; Thermo Fisher Scientific) at 50 °C with a flow rate of 400 μL min^{-1}. The mobile phases consisted of H_2O/CH_3COOH (99.85:0.15, *v/v*) with 5 mmol L^{-1} CH_3COONH_4 (phase A) and MeOH/*i*-PrOH/CH_3COOH (79.85:20.00:0.15, *v/v/v*) with 5 mmol L^{-1} CH_3COONH_4 (phase B). The chromatographic gradient was as follows: 1 min at 50 % phase B, from 50 to 70 % phase B in 4 min, from 70 to 99 % phase B in 18 min, 99 % phase B for 10 min (washing step), 99 to 50 % phase B in 1 min, and 50 % phase B for 8 min (equilibration step). The injection volume was 10 μL. The UHPLC system was coupled to the Q Exactive hybrid quadrupole-Orbitrap mass spectrometer (Thermo Fisher Scientific) by a heated electrospray source operated in negative ion mode (HESI−) using the following source settings: spray voltage 2.5 kV; capillary temperature 320 °C; sheath gas flow rate 35 arbitrary units (a.u.); auxiliary gas flow rate 25 a.u.; auxiliary gas heater temperature 400 °C. Full-scan MS data were acquired in the range of 200–1200 *m/z* with a resolution (full width at half-maximum, FWHM) of 35,000. The automatic gain control (AGC) target value was 500,000, the maximum ion injection time was 200 ms, and the isolation window width was 2 *m/z*. Top 5 data-dependent acquisition (DDA) MS/MS fragmentation was performed with a resolution (FWHM) of 17,500. AGC target value was set at 100,000, and dynamic exclusion was set to 2 s. Collision energy fragmentation was achieved in the HCD cell at 30 NCE. A process blank sample, obtained after a solvent sample was subject to the whole analytical platform, was analyzed together with the samples in order to remove the contaminants derived from both sample preparation and data acquisition. Raw data files were acquired by Xcalibur software (version 3.1, Thermo Fisher Scientific).

2.6. Lipid identification

For the identification of the polar lipidome of hempseeds, samples, and blanks were processed on Compound Discoverer (v. 3.1, Thermo Fisher Scientific) using a customized data processing workflow specifically dedicated to the tentative identification of fatty acids and polar lipids (Fig. S1). To this extent, a fatty acid and phospholipid mass list was built in Excel based on the LIPID MAPS database [28] for FA, GP, and sphingolipids. Feature alignment was obtained by the adaptive curve regression model; whenever the adaptive curve model failed, the linear model was automatically selected instead. After the alignment, adducts were detected and grouped, and the list of features was filtered to remove the ones whose areas in the process blank were more than 20 % of the average peak areas in the samples employing the tools “Fill Gaps” and “Mark Background Compounds”. Moreover, Compound Discoverer allowed the prediction of elemental compositions and the match of the extracted masses and elemental compositions to those present in the lipid mass list. To facilitate the manual annotation of lipids, a filter was enabled to remove all masses that were not present in the lipid database from the list of extracted features. Finally, filtered features were annotated by matching the experimental tandem mass spectra with open-access mass spectral databases and/or based on lipid fragmentation patterns [33–35]. To determine carbon−carbon double bonds on FA and fatty acyl chains in GP, aPB reaction products (corresponding to a relative mass shift of +113.0225) were manually searched in the MS data for all annotated lipids whose maximum peak area among the 27 samples was at least 10 times higher than that of the least abundant of the annotated underivatized lipids. Diagnostic product ions and relative abundances of the isomers were evaluated based on previous results [27].

2.7. Statistical analysis

MetaboAnalyst 5.0 was employed for comparing the five extraction procedures comparing the peak areas of the 16 monitored lipids after IS-based normalization [36]. The data matrix was submitted as a text file that was prepared according to the specific indications that are furnished by the developers. The interquartile range (IQR) was selected for data filtering, whereas the autoscaling algorithm was selected for data scaling. One-way analysis of variance (ANOVA) was performed to evaluate the lipid classes whose extraction was significantly affected by the tested procedures (p-value <0.001). A correlation heatmap was obtained to display the correlation among the lipid classes based on the different extraction procedures. Moreover, the data matrix obtained after the annotation of the underivatized FA and GP was submitted to MetaboAnalyst 5.0 [36] to obtain hierarchical clustering information (dendrogram and heatmap), principal component analysis (PCA), as well as a correlation heatmap of the annotated lipids in the nine analyzed hempseeds.

3. Results and discussion

3.1. Choice of the extraction protocol

Given the interesting nutritional properties of FA in hempseed and its derivatives [37], a large body of literature has dealt with the characterization of these compounds [38–45]. Much less is known, on the other hand, on the polar lipid composition of hempseeds [11,13,15] and a general consensus on the most efficient extraction techniques is still missing. Most previous studies have employed the widespread biphasic extraction mixtures based on halogenated solvents, such as the Folch [13,45] and the B&D [44] extractions, even though recent studies in lipidomics have highlighted the potential of greener monophasic approaches [46]. To gather information on the most suitable protocol for (i) maximizing the extraction efficiency and (ii) coupling the extraction with the subsequent aPB derivatization step, five different protocols were compared on a hempseed pooled sample: biphasic B&D and its green alternative Matyash extractions (protocols I and II) and monophasic extractions using the BuMe mixture [32] (protocol III), EtOH (protocol IV), and MeOH (protocol V). Protocols I-III were selected based on their well-known efficiency in extracting lipids from plant matrices [47], whereas protocols IV and V were selected for being extremely compatible with the aPB derivatization, which occurs in polar and protic solvents [27], as well as for their proven capacity to extract GP from biological matrices [48]. All protocols were applied with a sample-to-solvent ratio of 1:15 (*w/v*). The five protocols were then compared after LC-HRMS analysis by evaluating the peak areas of 16 selected lipids after IS-based normalization, i.e., 6 FA in a wide range of abundances (from low-abundance FA 20:1 to extremely abundant FA 18:2) and 5 pairs of GP of five subclasses (PA, PG, PE, PC, and PI). Fig. S2 summarizes the results of the 16 monitored lipids extracted by the 5 protocols (three experimental replicates per protocol). Saturated FA (SFA, FA 16:0, and FA 18:0) were more efficiently extracted by the BuMe and MeOH protocols, while the highest peak areas of unsaturated FA were obtained after EtOH and MeOH extractions. In general, the monophasic extractions granted higher extraction efficiency for FA that was rationalized based on the affinity of the free carboxyl group with the employed protic solvents. The BuMe extraction furnished the highest peak areas for all monitored zwitterionic GP (PC and PE), with protocols I, IV, and V evenly distributed in second place. On the other hand, anionic GP (PA, PG, and PI) were much more efficiently extracted by the monophasic protocols. The latter results can be attributed to a partial

distribution of the charged anionic GP in the aqueous phase compared to the globally neutral zwitterionic GP. The poor results obtained by the Matyash extraction (protocol II) for all monitored lipids could derive from the chosen sample-to-solvent ratio. It was demonstrated that for serum lipidomics, the Matyash extraction gave comparable results to Folch and B&D extraction only at the lowest sample-to-solvent ratio (1:100, *w/v*) [49]. ANOVA processing of the results demonstrated that all but one monitored lipids (PC 16:0_18:2) were significantly affected by the five tested protocols (Fig. S3), and the correlation heatmap confirmed the presence of three highly correlated subsets of lipids (FA, zwitterionic GP, and anionic GP, Fig. S4). A difference in the correlation coefficient between SFA and unsaturated FA is also clearly visible. The characteristics of the hempseed polar lipidome were also believed to significantly affect the results. The high abundance of free and conjugated PUFA, which are more polar than SFA and monounsaturated FA, were in fact believed to have played a major role in the overall better performance of protocols IV and V. These results are in agreement with previous findings by Höring [48], who demonstrated that one-phase alcoholic extractions are perfectly suitable for GP and much less efficient for GL. Considering the results on the monitored lipid and the facile coupling with the aPB derivatization, protocol V was chosen for hempseed untargeted polar lipidomics.

3.2. Untargeted lipidomics of hempseed extracts

Following lipid extraction and LC-HRMS analysis, underivatized FA and GP were annotated using Compound Discoverer, a data processing software specifically designed for HRMS data treatment for small molecules. The software is based on a system of nodes and blocks that can be customized when the analyses of specific classes of compounds are performed, thus removing background compounds, reducing the number of false positives, and aiding and streamlining the manual annotation. For FA and GP identification, a homemade lipid database was built based on the LIPID MAPS lipid classification [28]. In particular, one or two among 28 SFA and unsaturated FA were combined using Excel with the polar heads corresponding to six GP subclasses (PA, PC, PE, PG, PI, PS), taking into account O-acyl, O-alkyl, and O-alkenyl bounds. For PE, the N-acetylation of the free amino group was also considered. A list of 5830 lipids with their associated molecular formulas and exact masses was then uploaded to Compound Discoverer as a mass list. Once the masses were extracted from the datasets and aligned, and the adducts were annotated and grouped, the tool "Fill Gaps" was employed to find chromatographic peaks that were detected in some input files but not in others (including the process blank), possibly because of abundance below the detection threshold or irregular peak shape. The gap-filling process ensured proper background removal [50]. Later, the "Search Mass List" tool allowed automatic matching of the experimental masses to those present in the database, thus filtering out all other masses. Due to their quaternary ammonium, PC do not produce deprotonated ions but either interact with buffer modifiers (acetate or formate) or undergo in-source fragmentation with the loss of a methyl group in a rough ratio of 3:1 [51]. This peculiar ionization mechanism causes false attribution when software programs annotate the adducts and molecular formulas. To deal with this, the software was tricked by adding to the PC in the database an additional $C_2H_4O_2$ to their formulas and 60.02113 to their calculated masses, corresponding to the adduct $[M + AcOH - H]^-$. FA and GP were then manually annotated by inspection of the MS/MS spectra based on their well-known fragmentation pathways [33–35]. A total of 184 molecular lipids were annotated after manual inspection of the diagnostic product ion (Table S1), including 26 FA and 158 GP. Among the GP subclasses, PI were the most numerous with 33 annotated lipids (including 8 lyso-PI, LPI), followed by PE (29 annotated lipids including 7 lyso-PE, LPE), PG (22 annotated lipids including 2 lyso-PG, LPG), PC (20 annotated lipids including 5 lyso-PC, LPC), PA (10 annotated lipids including one lyso-PA, LPA), and PS (7 annotated lipids). Moreover, two uncommon classes of lipids were tentatively identified, i.e., N-acyl PE (NAPE, 27 lipids) and PA methyl esters (PAME, 8 lipids). Lipids belonging to the class of NAPE were previously reported in vegetable matrices [52,53] and are characterized by the N-acylation of a fatty acyl chain. The glycerol backbone of NAPE can present two fatty acyl chains, one fatty acyl chain (lyso-NAPE, L-NAPE), or no glycerol esters (N-acylglycerophosphoethanolamine, GP-NAE) [53]. Thus, L-NAPE and GP-NAE are isomers of PE and LPE, respectively, despite showing distinct fragmentation patterns. Due to the FA conjugation, the diagnostic peaks of the phosphoethanolamine head (*m/z* 140.0117 and 196.0379) are absent, and a much higher abundance of the glycerol phosphate is shown (*m/z* 152.9956), thus implying the preference for the cleavage of the phosphoester bond between the phosphate and the ethanolamine over the amide bond of the N-acyl conjugation (exemplary spectra are shown in Figs. S5a–b). As a consequence of this, GP-NAE did not show any ion corresponding to FA chains (Fig. S6). The elution order of the two classes also helped the assignment, with L-NAPE eluting earlier than PE due to the free hydroxyl group of the former (Fig. S7). A second peak was found in the case of two of the annotated L-NAPE. These two L-NAPE isomers had a similar fragmentation pattern to L-NAPE, except for the relative abundance of the ketene ions resulting from the loss of the FA chain (Fig. S5c). When one of the FA on the glycerol backbone of NAPE is hydrolyzed, the process might happen in both *sn*-1 and *sn*-2 positions, thus generating a pair of L-NAPE isomers. The uneven distribution of the two L-NAPE isomers could derive from a preference for the hydrolysis site in analogy with the hydrolysis processes from GP that generate their lyso forms. PAME have been previously reported as artifacts deriving from the lipid extraction process of microgreen crops [54]. Despite not being included in the lipid database, their identification could still be carried out since the software associated their masses with those of PA with a longer FA. The identification of PAME was based on two diagnostic product ions with a mass shift of 14.0156 (CH_2) compared to the corresponding ions of PA, i.e., *m/z* 110.9852, corresponding to methylated phosphoric acid, and *m/z* 167.0113, corresponding to methylated glycerol phosphate (Fig. S8).

3.3. Regioisomeric distribution of carbon-carbon double bonds

Due to the nutritional and biological implications of carbon-carbon double bonds on FA and GP [8–10], the derivatization procedure was carried out on the hempseed methanol extracts based on an aPB reaction that allows pinpointing the double bonds in HESI− [27]. The chosen extraction protocol using pure MeOH allowed direct derivatization without the need for the removal of the extraction solvent, thus avoiding time-consuming steps that could also result in the partial loss of the analytes. The aPB reaction is a photochemical [2 + 2] cycloaddition between the double bonds of free and conjugated FA and the imine group of the 6-AU reactant with estimated yields of around 20–30 % regardless of the nature of the lipid, in line with previous findings of other PB reactions [20,21]. The azetidine rings resulting from the reaction undergo cleavage under HCD fragmentation that allows pinpointing the original position of the carbon-carbon double bond. For example, regioisomers of FA 18:1 with the double bond in ω-9 (oleic acid, OA) and ω-7 (vaccenic acid, VA) produce distinct MS/MS spectra, with the former generating two ions at *m/z* 223.1446 and 182.1179 (Fig. 1a) and the latter generating two ions at *m/z* 195.1132 and 210.1494 (Fig. 1b). As such, the relative abundances of FA isomers can be calculated by comparing the diagnostic ions in the MS/MS spectra of the lipid extracts after derivatization (Fig. 1c) through linear regressions that were previously obtained for the analytical standards of the pairs of isomers of FA 18:1 and 18:3 at different ratios and fixed combined concentration [27]. For the other FA, the double bond position was determined with the same rationale, keeping in mind that two diagnostic ions are generated for each double bond position, i.e., six ions for α-linolenic acid (ALA, ω-3) and γ-linolenic acid (GLA, ω-6). Because the abundance of the diagnostic ions decreases with their number, only the most intense one (i.e., the odd mass ion) was considered for each pair.

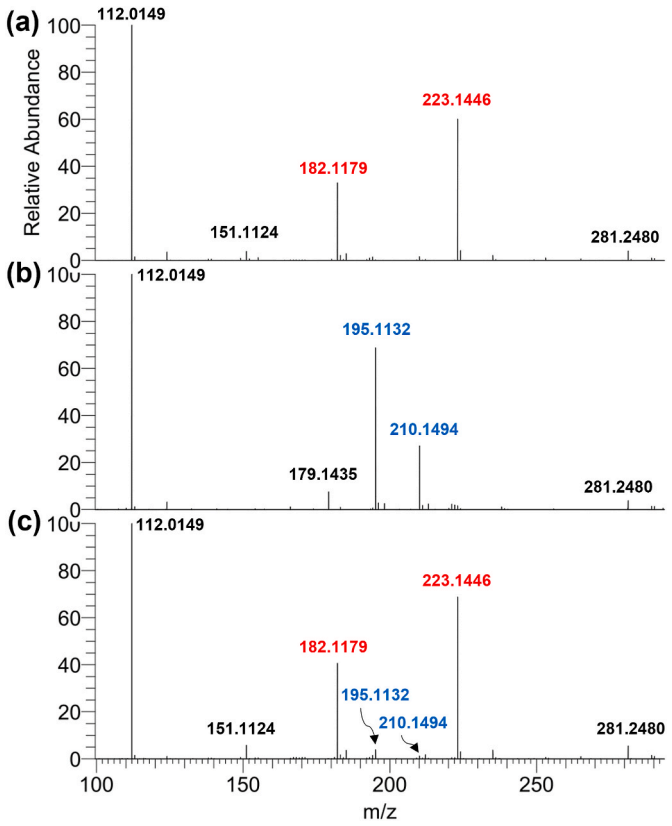

Fig. 1. MS/MS spectra associated to *m/z* 394.2707 in ESI− of (a) the aPB derivative of analytical standard oleic acid (FA 18:1 ω-9), (b) the aPB derivative of analytical standard vaccenic acid (FA 18:1 ω-7), and (c) the aPB derivative of FA 18:1 from hempseed lipid extract.

Following the aPB derivatization, two pairs of isomers were identified for octadecenoic and octadecatrienoic acid, i.e., OA/VA and ALA/GLA (Fig. S9b). Whereas the ALA/GLA pair has been extensively studied for its bioactive properties, VA has been measured in hempseed oil by targeted GC approaches [55]. Traces of FA 18:2 ω-8 were also annotated for some of the varieties along with the major linoleic acid (FA 18:2 ω-6, Fig. S9a) thanks to the two diagnostic ions (*m/z* 249.1605 and 209.1301 vs *m/z* 221.1298 and 191.0983). On the other hand, octadecatetraenoic and eicosenoic acid were only found as the ω-3 (stearidonic acid) and ω-9 (gondoic acid) regioisomers, respectively. The results on FA 20:1 (Fig. S9c) are not surprising, given that gondoic acid was previously found in nuts [56], whereas the two other known isomers (ω-11 and ω-7) are typical of animals [57] and plants [58]. For some of the analyzed strains, it was also possible to determine the regioisomeric distribution of FA 16:1 and 20:2, which always resulted in ω-7 (palmitoleic acid) and ω-6, respectively. Double bonds undergo aPB derivatization both on free FA and those bound to GP, allowing the determination of their regiochemistry on all classes of analyzed lipids except GP-NAE, that do not present conjugations on the glycerol backbone and, subsequently, FA product ions. Due to their quaternary ammonium group, PC undergo a methyl transfer from the polar head to the 6-AU moiety when their derivatives are subject to ESI− ionization [27]. Thus, diagnostic ions of PC have a mass shift of 14.0156, which corresponds to an extra CH_2, i.e., 237.1612 vs 223.1446 for oleic acid. It is important to highlight that the ALA/GLA ratio could not be calculated for GP bound to one FA 18:2 and one FA 18:3, since the product ions of linoleic acid (*m/z* 181.0983 and 221.1298) are in common with GLA (*m/z* 181.0983, 221.1298, and 261.1602). For the regioisomers to be evaluated, the limiting factor was the abundance of the underivatized lipid in the extracts. Due to the yields obtained by photochemical [2 + 2] reactions (estimated around 20–25 % in our previous work for aPB [27] and by Zhao for PB [21]), only the lipid species whose areas were around ten times higher than the least abundant annotated lipid from the hempseed extracts produced the diagnostic MS/MS spectra. Moreover, 31 lipids had to be excluded because comprised only SFA, as well as the 4 annotated GP-NAE. The lipids whose double bond positions were determined through inspection of the MS/MS spectra of the aPB derivatives are listed in Table S2.

3.4. Lipid profile of the hempseed varieties

To assess the polar lipidome of hempseeds of the varieties grown in the European Union, 7 different varieties (Carmaleonte, Eletta Campana, Ermo, FINOLA, Futura 75, Santhica 27, and USO 31) and 2 accessions (Felsinea and S435) were analyzed by the setup extraction, derivatization, and HRMS workflow. For each strain, three distinct samples were subject to the whole workflow. To the best of our knowledge, this is the first comprehensive characterization of the polar lipidome in raw hempseeds, whereas some previous papers have characterized polar lipids from hempseed derivatives and by-products, such as oil [15], cakes [13], and residual biomass [59]. Twenty-six FA were annotated, the shortest being myristic acid (FA 14:0) and the longest being melissic acid (FA 30:0) (Table S1). In Table 1, the relative abundances of FA in the 9 varieties are reported after normalization using the IS. Unsurprisingly, linoleic acid was the most abundant for all varieties, comprising 40–57 % of the total FA content, followed by octadecenoic (OA + VA, FA 18:1), linolenic (ALA + GLA, FA 18:3), and palmitic acid (FA 16:0) with 11.5–25.1 %, 7.7–17.0 %, and 5.3–7.9 %, respectively. Among the other constituents, stearic acid (FA 18:0) comprised around 3–4% of the total FA content, followed by several other constituents at around 1 %, i.e., stearidonic acid (FA 18:4), arachidic acid (FA 20:0), gondoic acid (FA 20:1), behenic acid (FA 20:0), lignoceric acid (FA 24:0), cerotic acid (FA 26:0), and montanic acid (FA 28:0). In analogy with previous findings [60], PUFA comprised around 70 % of the total FA content for all analyzed hempseed varieties except Felsinea (52 %), which in turn had the maximum content of SFA (22.9 %). Similar PUFA/SFA ratios were calculated for most strains (4–5.5), except for S435 at 3.2 and Felsinea at 2.3. The total ω-6 content, i.e., the combined abundance of linoleic acid, GLA, and eicosadienoic acid, was comprised between 46 % and 61 %, whereas the total ω-3 content, i.e., ALA and stearidonic acid, was between 7.5 and 16 %, resulting in ω-6/ω-3 ratios between 3.5 and 4.7 for most varieties except for FINOLA at 5.6 and Carmaleonte at 7.2. Coherently with the most dramatic differences being related to single FA rather than FA classes, the aPB derivatization allowed the discovery of interesting differences in the OA/VA and ALA/GLA ratios among the analyzed varieties, the former being comprised between 8 and 28 and the latter between 1.7 and 28. Such differences are in agreement with previous results on different strains that might appear contradictory, but that rather displayed the intra-strain variability of hempseeds. A previous GC-based study on 13 commercial hempseed oils from unknown varieties measured ALA/GLA ratios ranging from 3 to 16 [60]. In 2022, two studies on hempseed oil from Futura 75 by Tura [55] and Occhiuto [61] measured ALA/GLA ratios of around 15 and 8, respectively, in good agreement with our results of 10. On the other hand, previous results from Irakli [62] on hempseeds of FINOLA and Santhica 27 varieties measured ALA/GLA ratios around 3 and 4, respectively, again in good agreement with our results of 1.7 and 3.3. As previously mentioned, the GP composition of hempseeds has been rarely investigated. In this work, a comprehensive phospholipidome characterization of the 9 hempseed varieties was achieved, filling a gap in the knowledge on the composition of such interesting novel foods. Fig. 2 shows the results for the 8 annotated lipids classes in terms of percentages (Fig. 2a) and absolute abundances (Fig. 2b). For the different classes to be compared, previous normalization using the Splash Lipidomix IS was performed, thus correcting the peak areas between the different lipid classes as well as between different samples over time, allowing an estimate of the relative abundances of the lipid classes. Due to the absence of class-specific IS, the

Table 1
Fatty acid composition of the nine analyzed hempseed varieties after methanol extraction and HRMS analysis. OA/VA and ALA/GLA ratios were calculated by comparison of the diagnostic ions obtained following aPB derivatization and MS/MS fragmentation.

Compound	Carmaleonte	Eletta Campana	Ermo	Felsinea	FINOLA	Futura 75	S435	Santhica 27	USO 31
	%	%	%	%	%	%	%	%	%
FA (16.0)	5.3 ± 0.1	5.8 ± 0.1	5.9 ± 0.3	7.9 ± 0.2	7.0 ± 0.1	6.8 ± 0.4	6.3 ± 0.5	7.1 ± 0.2	6.4 ± 0.2
FA (18:0)	3.11 ± 0.03	3.3 ± 0.1	2.75 ± 0.04	4.7 ± 0.3	3.6 ± 0.1	4.0 ± 0.2	3.9 ± 0.1	3.7 ± 0.2	3.6 ± 0.1
FA (18:1)[a]	25.1 ± 0.6	14.8 ± 0.1	12.3 ± 0.6	23.1 ± 0.6	11.5 ± 0.2	14.0 ± 0.6	15 ± 1	12.8 ± 0.5	12.7 ± 0.2
FA (18:2)	54 ± 2	54 ± 3	57.3 ± 0.7	40 ± 1	55 ± 1	55 ± 2	50 ± 2	53 ± 1	53 ± 1
FA (18:3)[b]	7.7 ± 0.1	16 ± 1	14.8 ± 0.7	11.9 ± 0.3	15 ± 1	12.4 ± 0.4	14.1 ± 0.1	15 ± 1	17 ± 2
FA (18:4)	0.22 ± 0.01	0.34 ± 0.01	1.17 ± 0.01	0.14 ± 0.01	1.7 ± 0.1	0.70 ± 0.02	0.25 ± 0.01	1.26 ± 0.02	1.32 ± 0.03
FA (20:0)	1.20 ± 0.01	1.20 ± 0.01	0.94 ± 0.04	1.46 ± 0.02	1.46 ± 0.03	1.05 ± 0.04	1.3 ± 0.1	1.11 ± 0.01	1.28 ± 0.05
FA (20:1)	0.74 ± 0.01	0.57 ± 0.01	0.51 ± 0.01	0.55 ± 0.01	0.62 ± 0.01	0.41 ± 0.02	0.45 ± 0.01	0.47 ± 0.01	0.66 ± 0.01
FA (22:0)	0.98 ± 0.01	0.98 ± 0.04	0.83 ± 0.01	1.75 ± 0.03	1.48 ± 0.03	1.21 ± 0.04	1.9 ± 0.1	1.03 ± 0.04	1.26 ± 0.02
FA (24:0)	0.69 ± 0.02	0.94 ± 0.03	1.06 ± 0.05	2.5 ± 0.2	1.18 ± 0.04	1.32 ± 0.04	2.0 ± 0.1	1.30 ± 0.03	0.99 ± 0.02
FA (26:0)	0.34 ± 0.01	0.56 ± 0.01	0.98 ± 0.04	1.92 ± 0.04	0.50 ± 0.01	1.08 ± 0.03	2.0 ± 0.1	0.93 ± 0.05	0.43 ± 0.01
FA (28:0)	0.26 ± 0.01	0.48 ± 0.01	0.45 ± 0.01	1.07 ± 0.03	0.13 ± 0.01	0.72 ± 0.02	1.60 ± 0.04	0.60 ± 0.02	0.21 ± 0.01
Others	0.90 ± 0.03	1.15 ± 0.04	1.04 ± 0.01	3.1 ± 0.3	1.25 ± 0.01	1.26 ± 0.05	1.8 ± 0.1	1.4 ± 0.1	1.20 ± 0.02
SFA	12.4 ± 0.1	14.0 ± 0.3	13.4 ± 0.3	22.9 ± 0.9	16.0 ± 0.2	16.9 ± 0.7	20.1 ± 0.7	16.6 ± 0.5	14.9 ± 0.2
MUFA	26.2 ± 0.6	15.7 ± 0.2	13.2 ± 0.6	25.0 ± 0.7	12.5 ± 0.2	14.8 ± 0.6	16 ± 1	13.7 ± 0.5	13.7 ± 0.3
PUFA	62 ± 2	70 ± 4	73 ± 1	52 ± 1	71 ± 2	68 ± 2	64 ± 2	70 ± 2	71 ± 2
ω6	54 ± 2	55 ± 3	59 ± 1	46 ± 1	61 ± 2	56 ± 2	51 ± 2	57 ± 1	56 ± 1
ω3	7.5 ± 0.1	16 ± 1	14.2 ± 0.6	11.5 ± 0.3	10.8 ± 0.7	12.0 ± 0.4	13.8 ± 0.1	12.8 ± 0.9	16 ± 2
OA/VA	8 ± 2	28 ± 4	9 ± 2	19 ± 3	8 ± 1	11 ± 2	15 ± 4	8 ± 1	11 ± 1
ALA/GLA	19 ± 3	19 ± 5	8 ± 2	19 ± 4	1.7 ± 0.3	10 ± 1	28 ± 3	3.3 ± 0.7	5 ± 2
PUFA/SFA	5.0 ± 0.2	5.0 ± 0.4	5.5 ± 0.1	2.3 ± 0.1	4.5 ± 0.2	4.0 ± 0.3	3.2 ± 0.2	4.2 ± 0.4	4.8 ± 0.2
ω6/ω3	7.2 ± 0.4	3.5 ± 0.4	4.2 ± 0.2	4.0 ± 0.2	5.6 ± 0.5	4.7 ± 0.3	3.7 ± 0.2	4.5 ± 0.4	3.6 ± 0.5

[a] OA + VA.
[b] ALA + GLA.

normalization of NAPE and PAME was obtained by employing PE and PA, respectively. For all cultivars, PI were the most abundant compounds, followed by PC, PE, and PG, with these four classes comprising up to 95 % of the total GP content. Except for PS, the minor classes of GP exhibited much greater variability; PA ranged between 0.9 % (Felsinea) and 5.9 % (USO 31), PAME were found between 0.1 % (most strains) and 6.2 % (USO 31), and NAPE were between 2.5 % (Felsinea) and 9.5 % (FINOLA). Based on the profiles shown in Fig. 2, FINOLA, USO 31, and, to a lower extent, Carmagnola stood out among all other classes, with a lower overall content of the major lipid classes and a higher content of PA, PAME, and NAPE. An increasing abundance of NAPE seemed correlated with a lower abundance of PE, from which they are known to originate in response to abiotic and biotic stress [52]. In terms of functional compounds, NAPE are of particular interest since they generate N-acylethanolamines, a class of bioactive compounds known for exerting physiological effects on the endocannabinoid signaling system [63]. On the other hand, PAME are not enzymatically produced by the plant but they are rather artifacts generated during extraction procedures that employ MeOH [54], an assumption that was confirmed by comparing the total ion current associated with these compounds after extraction of the hempseed pool with or without methanol (Fig. S10). The differences in the abundance of PAME among the samples can be attributed to the presence of specific phospholipases that are known to convert GP to PAME in some of the analyzed strains [54].

Unsurprisingly, the FA bound to the annotated GP mirrored the annotated free FA, with a high prevalence of chains with 18 and 16 carbon atoms, whereas few lipids, in prevalence zwitterionic PE and PC, exhibited longer FA chains. On the other hand, the annotated PG and PI had a higher prevalence of short and saturated chains, including odd-numbered 15:0 and 17:0. The aPB derivatization of the hempseed extracts allowed the determination of the regiochemistry of FA chains bound to GP with the same rationale of free FA when the abundance of the compounds allowed the MS/MS fragmentation of the derivatized lipids (69 sum compositions, Table S2). Because of the FA composition of the annotated GP, the regiochemistry of esterified FA 18:1, 18:2, and 18:3 was determined regardless of the nature of the GP class, thus demonstrating the applicability of the aPB reaction for all analyzed lipid classes. The results obtained for esterified FA mirrored those of the free ones, with strains with lower OA/VA and ALA/GLA ratios exhibiting the highest abundances of the minor isomers. Among the GP classes, zwitterionic PC and PE exhibited a higher content of minor FA regioisomers compared to anionic PG and PI, confirming a rather different profile of the conjugated FA between the two classes. The data matrix of the annotated lipids was then subject to hierarchical clustering analysis using MetaboAnalysist. Fig. S11 shows hierarchical clustering heatmaps and dendrograms using all variables (Fig. S11a) and the most significant 75 lipids from ANOVA analysis (Fig. S11b) for improved readability. Both hierarchical clustering analyses furnished analog dendrogram results, with two main hempseed clusters, one constituted by Carmagnola, FINOLA, and USO 31 and one by the six others. Most GP classes had consistently lower abundance in the cluster of Carmagnola, FINOLA, and USO 31, which had in turn a generally higher abundance of FA and PA. USO 31 had the highest abundance of PAME and L-NAPE, whereas FINOLA had the maximum concentration of NAPE. Among the individual strains, Ermo stood out for its content in lyso-GP, whereas Felsinea for its content in some PC, PE, and PS bound to linoleic acid. The dendrogram results were confirmed by the PCA, an unsupervised multivariate statistical approach employing the annotated lipids as variables. As shown in Fig. S12, Carmagnola, FINOLA, and USO 31 had negative values of PC1, which explained 35.3 % of the total variance, while the other cluster of six samples had positive values. Moreover, alongside PC2, Felsinea and Ermo stood out from the second cluster, with positive and negative values, respectively, whereas the four remaining had values around zero. Finally, a correlation heatmap was obtained (Fig. S13) to evaluate the correlation among the annotated lipids based on the content in the 9 analyzed varieties. Unsurprisingly, some lipid classes were highly correlated, such as FA, PAME, and NAPE (correlation factors above 0.7). Moreover, lyso-GP of different classes were highly correlated, implying that their generation by phospholipases is non-specific to the class. An interesting result was found on GP bound to ALA/GLA regardless of the subclass, which had extremely high correlation factors with each other but were much less correlated with the other GP. It is known that PUFA are preferably linked to the *sn*-2 position of the phosphoglycerol backbone and that the remodeling of the linkage to that position is governed by the enzymes involved in the so-called Lands' Cycle [64]. As such, it is possible to hypothesize that linolenic acid conjugation is governed by the sequential activity of phospholipase A2 and lysophospholipid acyltransferase, which

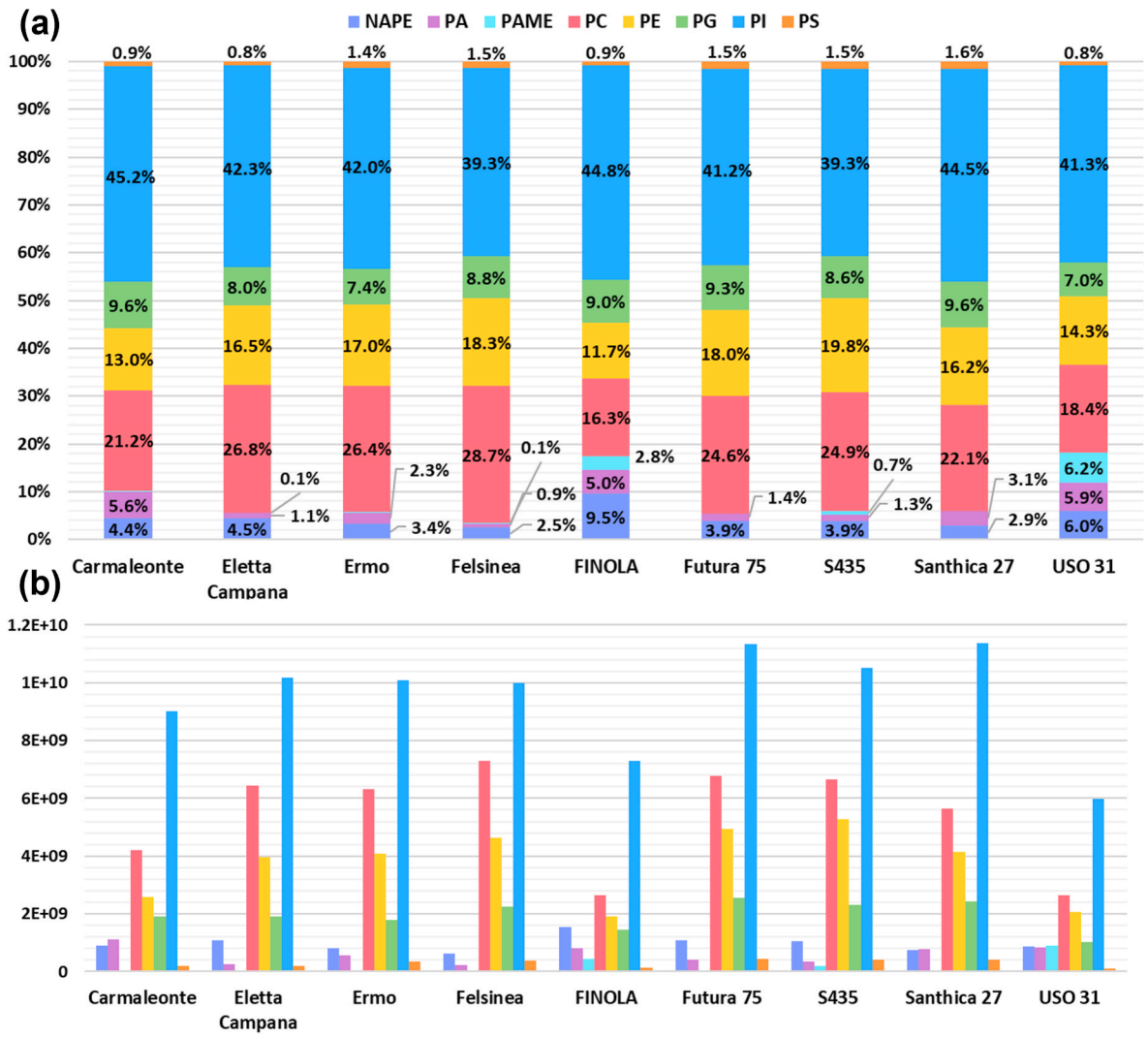

Fig. 2. Comparison of the lipid class content in the nine analyzed hempseed samples in terms of (a) relative abundances and (b) absolute peak areas after IS-based normalization.

hydrolyze and reacylate the *sn*-2 position of GP.

4. Conclusions

The consumption of hempseeds and its derivatives is rapidly increasing for the high nutritional value of its bioactive compounds, including a rich lipidome with elevated concentrations in PUFA with optimum ω-6/ω-3 ratio. Despite this, comprehensive characterization of the polar lipidome where missing, especially regarding the regioisomer composition of FA bound to GP. The proposed methodology, which coupled monophasic extraction with direct aPB derivatization, allowed the HRMS-based untargeted characterization of the whole polar lipidome, including minor lipid classes and FA regioisomers. Monophasic extractions were found perfectly suitable for lipid extraction, with comparable or even exceeding results compared to standard two-phase protocols. The one-phase extraction with MeOH was not merely greener, cheaper, and faster, but allowed also a direct photochemical reaction. In these regards, the aPB reaction proved its analytical potential despite dealing with a complex matrix enriched with lipids containing FA chains with two or more unsaturations. The characterization of the polar lipidome of nine of the hempseeds that are cultivated in the EU demonstrated the rich content in biologically active free and conjugated PUFA, as well as significant intra-strain differences in terms of both lipid composition and minor regioisomer content. Thanks to the aPB derivatization, the relative quantitation of regioisomers was possible without the need for analytical standards or other analytical techniques. Further studies are needed to test the biological potential of the lipid extracts to evaluate differences based on the individual lipid composition of each hempseed cultivar.

CRediT authorship contribution statement

Andrea Cerrato: Writing – original draft, Methodology, Formal analysis. **Sara Elsa Aita:** Investigation. **Giuseppe Cannazza:** Supervision, Resources. **Chiara Cavaliere:** Writing – review & editing. **Alberto Cavazzini:** Supervision. **Cinzia Citti:** Writing – review & editing, Investigation. **Carmela Maria Montone:** Writing – review & editing, Supervision, Conceptualization. **Enrico Taglioni:** Visualization, Investigation. **Aldo Laganà:** Project administration, Conceptualization.

Declaration of competing interest

The authors declare that they have no known competing financial interests or personal relationships that could have appeared to influence the work reported in this paper.

Data availability

Data will be made available on request.

Acknowledgments

The authors thank Dr. Massimo Montanari from CREA-CI for developing the two accessions used in this work and Dr. Roberta Paris for providing all the hempseeds samples.

Appendix A. Supplementary data

Supplementary data to this article can be found online at https://doi.org/10.1016/j.talanta.2024.125686.

References

[1] A.G. Duque Schumacher, S. Pequito, J. Pazour, Industrial hemp fiber: a sustainable and economical alternative to cotton, J. Clean. Prod. 268 (2020) 122180, https://doi.org/10.1016/j.jclepro.2020.122180.
[2] European Commission, COUNCIL DIRECTIVE 2002/53/EC of 13 June 2002 on the common catalogue of varieties of agricultural plant species, Off. J. Eur. Union (2002) 1–8.
[3] S.O. Aloo, G. Mwiti, L.W. Ngugi, D.-H. Oh, Uncovering the secrets of industrial hemp in food and nutrition: the trends, challenges, and new-age perspectives, Crit. Rev. Food Sci. Nutr. (2022) 1–20, https://doi.org/10.1080/10408398.2022.2149468.
[4] J.C. Callaway, Hempseed as a nutritional resource: an overview, Euphytica 140 (2004) 65–72, https://doi.org/10.1007/s10681-004-4811-6.
[5] G. Santos-Sánchez, A.I. Álvarez-López, E. Ponce-España, A. Carrillo-Vico, C. Bollati, M. Bartolomei, C. Lammi, I. Cruz-Chamorro, Hempseed (Cannabis sativa) protein hydrolysates: a valuable source of bioactive peptides with pleiotropic health-promoting effects, Trends Food Sci. Technol. (2022), https://doi.org/10.1016/j.tifs.2022.06.005.
[6] A. Cerrato, C. Lammi, A. Laura Capriotti, C. Bollati, C. Cavaliere, C. Maria Montone, M. Bartolomei, G. Boschin, J. Li, S. Piovesana, A. Arnoldi, A. Laganà, Isolation and functional characterization of hemp seed protein-derived short- and medium-chain peptide mixtures with multifunctional properties for metabolic syndrome prevention, Food Res. Int. 163 (2023) 112219, https://doi.org/10.1016/j.foodres.2022.112219.
[7] R.K. Saini, Y.-S. Keum, Omega-3 and omega-6 polyunsaturated fatty acids: dietary sources, metabolism, and significance — a review, Life Sci. 203 (2018) 255–267, https://doi.org/10.1016/j.lfs.2018.04.049.
[8] Y. Adkins, D.S. Kelley, Mechanisms underlying the cardioprotective effects of omega-3 polyunsaturated fatty acids, J. Nutr. Biochem. 21 (2010) 781–792, https://doi.org/10.1016/j.jnutbio.2009.12.004.
[9] E.A. Dennis, P.C. Norris, Eicosanoid storm in infection and inflammation, Nat. Rev. Immunol. 15 (2015) 511–523, https://doi.org/10.1038/nri3859.
[10] J.X. Kang, A. Liu, The role of the tissue omega-6/omega-3 fatty acid ratio in regulating tumor angiogenesis, Cancer Metastasis Rev. 32 (2013) 201–210, https://doi.org/10.1007/s10555-012-9401-9.
[11] C. Lopez, B. Novales, H. Rabesona, M. Weber, T. Chardot, M. Anton, Deciphering the properties of hemp seed oil bodies for food applications: lipid composition, microstructure, surface properties and physical stability, Food Res. Int. 150 (2021) 110759, https://doi.org/10.1016/j.foodres.2021.110759.
[12] K. Lane, E. Derbyshire, W. Li, C. Brennan, Bioavailability and potential uses of vegetarian sources of omega-3 fatty acids: a review of the literature, Crit. Rev. Food Sci. Nutr. 54 (2014) 572–579, https://doi.org/10.1080/10408398.2011.596292.
[13] C. Buré, A. Solgadi, S. Yen-Nicolaÿ, T. Bardeau, D. Libong, S. Abreu, P. Chaminade, P. Subra-Paternault, M. Cansell, Electrospray mass spectrometry as a tool to characterize phospholipid composition of plant cakes, Eur. J. Lipid Sci. Technol. 118 (2016) 1282–1292, https://doi.org/10.1002/ejlt.201500345.
[14] A. Kozub, H. Nikolaichuk, K. Przykaza, J. Tomaszewska-Gras, E. Fornal, Lipidomic characteristics of three edible cold-pressed oils by LC/Q-TOF for simple quality and authenticity assurance, Food Chem. 415 (2023) 135761, https://doi.org/10.1016/j.foodchem.2023.135761.
[15] I. Bakhytkyzy, W. Hewelt-Belka, A. Kot-Wasik, A comprehensive lipidomic analysis of oilseeds using LC-Q-TOF-MS and dispersive micro-solid phase (D-μ-SPE) extraction techniques, J. Food Compos. Anal. 116 (2023) 105037, https://doi.org/10.1016/j.jfca.2022.105037.
[16] C. Bielow, G. Mastrobuoni, M. Orioli, S. Kempa, On mass ambiguities in high-resolution shotgun lipidomics, Anal. Chem. 89 (2017) 2986–2994, https://doi.org/10.1021/acs.analchem.6b04456.
[17] J.R. Bonney, B.M. Prentice, Perspective on emerging mass spectrometry technologies for comprehensive lipid structural elucidation, Anal. Chem. 93 (2021) 6311–6322, https://doi.org/10.1021/acs.analchem.1c00061.
[18] M.C. Thomas, T.W. Mitchell, D.G. Harman, J.M. Deeley, J.R. Nealon, S.J. Blanksby, Ozone-induced dissociation: elucidation of double bond position within mass-selected lipid ions, Anal. Chem. 80 (2008) 303–311, https://doi.org/10.1021/ac7017684.
[19] L.A. Macias, K.Y. Garza, C.L. Feider, L.S. Eberlin, J.S. Brodbelt, Relative quantitation of unsaturated phosphatidylcholines using 193 nm ultraviolet photodissociation parallel reaction monitoring mass spectrometry, J. Am. Chem. Soc. 143 (2021) 14622–14634, https://doi.org/10.1021/jacs.1c05295.
[20] X. Ma, L. Chong, R. Tian, R. Shi, T.Y. Hu, Z. Ouyang, Y. Xia, Identification and quantitation of lipid C=C location isomers: a shotgun lipidomics approach enabled by photochemical reaction, Proc. Natl. Acad. Sci. USA 113 (2016) 2573–2578, https://doi.org/10.1073/pnas.1523356113.
[21] J. Zhao, X. Xie, Q. Lin, X. Ma, P. Su, Y. Xia, Next-generation paternò–büchi reagents for lipid analysis by mass spectrometry, Anal. Chem. 92 (2020) 13470–13477, https://doi.org/10.1021/acs.analchem.0c02896.
[22] F. Tang, C. Guo, X. Ma, J. Zhang, Y. Su, R. Tian, R. Shi, Y. Xia, X. Wang, Z. Ouyang, Rapid in situ profiling of lipid C=C location isomers in tissue using ambient mass spectrometry with photochemical reactions, Anal. Chem. 90 (2018) 5612–5619, https://doi.org/10.1021/acs.analchem.7b04675.
[23] Z. Li, S. Cheng, Q. Lin, W. Cao, J. Yang, M. Zhang, A. Shen, W. Zhang, Y. Xia, X. Ma, Z. Ouyang, Single-cell lipidomics with high structural specificity by mass spectrometry, Nat. Commun. 12 (2021) 2869, https://doi.org/10.1038/s41467-021-23161-5.
[24] Q. Lin, P. Li, M. Fang, D. Zhang, Y. Xia, Deep profiling of aminophospholipids reveals a dysregulated desaturation pattern in breast cancer cell lines, Anal. Chem. 94 (2022) 820–828, https://doi.org/10.1021/acs.analchem.1c03494.
[25] Z. Liu, S. Rochfort, Regio-distribution and double bond locations of unsaturated fatty acids in phospholipids of bovine milk, Food Chem. 373 (2022) 131515, https://doi.org/10.1016/j.foodchem.2021.131515.
[26] D. Coniglio, G. Ventura, C.D. Calvano, I. Losito, T.R.I. Cataldi, Positional assignment of C−C double bonds in fatty acyl chains of intact arsenosugar phospholipids occurring in seaweed extracts by epoxidation reactions, J. Am. Soc. Mass Spectrom. 33 (2022) 823–831, https://doi.org/10.1021/jasms.2c00006.
[27] A. Cerrato, A.L. Capriotti, C. Cavaliere, C.M. Montone, S. Piovesana, A. Laganà, Novel aza-paternò-büchi reaction allows pinpointing carbon–carbon double bonds in unsaturated lipids by higher collisional dissociation, Anal. Chem. 94 (2022) 13117–13125, https://doi.org/10.1021/acs.analchem.2c02549.
[28] E. Fahy, S. Subramaniam, H.A. Brown, C.K. Glass, A.H. Merrill, R.C. Murphy, C.R. H.H. Raetz, D.W. Russell, Y. Seyama, W. Shaw, T. Shimizu, F. Spener, G. van Meer, M.S. VanNieuwenhze, S.H. White, J.L. Witztum, E.A. Dennis, A comprehensive classification system for lipids, J. Lipid Res. 46 (2005) 839–861, https://doi.org/10.1194/jlr.E400004-JLR200.
[29] G. Liebisch, J.A. Vizcaíno, H. Köfeler, M. Trötzmüller, W.J. Griffiths, G. Schmitz, F. Spener, M.J.O. Wakelam, Shorthand notation for lipid structures derived from mass spectrometry, J. Lipid Res. 54 (2013) 1523–1530, https://doi.org/10.1194/jlr.M033506.
[30] E.G. Bligh, W.J. Dyer, A rapid method of total lipid extraction and purification, Can. J. Biochem. Physiol. 37 (1959) 911–917, https://doi.org/10.1139/o59-099.
[31] V. Matyash, G. Liebisch, T.V. Kurzchalia, A. Shevchenko, D. Schwudke, Lipid extraction by methyl-tert-butyl ether for high-throughput lipidomics, J. Lipid Res. 49 (2008) 1137–1146, https://doi.org/10.1194/jlr.D700041-JLR200.
[32] L. Löfgren, G.-B. Forsberg, M. Ståhlman, The BUME method: a new rapid and simple chloroform-free method for total lipid extraction of animal tissue, Sci. Rep. 6 (2016) 27688, https://doi.org/10.1038/srep27688.
[33] J. Pi, X. Wu, Y. Feng, Fragmentation patterns of five types of phospholipids by ultra-high-performance liquid chromatography electrospray ionization quadrupole time-of-flight tandem mass spectrometry, Anal. Methods 8 (2016) 1319–1332, https://doi.org/10.1039/C5AY00776C.
[34] J.P. Koelmel, N.M. Kroeger, C.Z. Ulmer, J.A. Bowden, R.E. Patterson, J.A. Cochran, C.W.W. Beecher, T.J. Garrett, R.A. Yost, LipidMatch: an automated workflow for rule-based lipid identification using untargeted high-resolution tandem mass spectrometry data, BMC Bioinf. 18 (2017) 331, https://doi.org/10.1186/s12859-017-1744-3.
[35] L. Zhou, F. Yang, M. Zhao, M. Zhang, J. Liu, E. Marchioni, Determination and comparison of phospholipid profiles in eggs from seven different species using UHPLC-ESI-Triple TOF-MS, Food Chem. 339 (2021) 127856, https://doi.org/10.1016/j.foodchem.2020.127856.
[36] J. Xia, D.S. Wishart, Metabolomic data processing, analysis, and interpretation using MetaboAnalyst, Curr. Protoc. Bioinforma. 34 (2011), https://doi.org/10.1002/0471250953.bi1410s34.
[37] J.I. Alonso-Esteban, J. Pinela, A. Ćirić, R.C. Calhelha, M. Soković, I.C.F.R. Ferreira, L. Barros, E. Torija-Isasa, M. de C. Sánchez-Mata, Chemical composition and biological activities of whole and dehulled hemp (Cannabis sativa L.) seeds, Food Chem. 374 (2022) 131754, https://doi.org/10.1016/j.foodchem.2021.131754.
[38] F. Anwar, S. Latif, M. Ashraf, Analytical characterization of hemp (Cannabis sativa) seed oil from different agro-ecological zones of Pakistan, J. Am. Oil Chem. Soc. 83 (2006) 323–329, https://doi.org/10.1007/s11746-006-1207-x.
[39] M. Kiralan, V. Gül, S. Metin Kara, Fatty acid composition of hempseed oils from different locations in Turkey, Spanish J. Agric. Res. 8 (2010) 385, https://doi.org/10.5424/sjar/2010082-1220.
[40] E. Vonapartis, M.-P. Aubin, P. Seguin, A.F. Mustafa, J.-B. Charron, Seed composition of ten industrial hemp cultivars approved for production in Canada, J. Food Compos. Anal. 39 (2015) 8–12, https://doi.org/10.1016/j.jfca.2014.11.004.
[41] J. Liang, A. Appukuttan Aachary, U. Thiyam-Holländer, Hemp seed oil: minor components and oil quality, Lipid Technol. 27 (2015) 231–233, https://doi.org/10.1002/lite.201500050.
[42] J.I. Alonso-Esteban, M.J. González-Fernández, D. Fabrikov, E. Torija-Isasa, M. de C. Sánchez-Mata, J.L. Guil-Guerrero, Hemp (cannabis sativa L.) varieties: fatty acid

profiles and upgrading of γ-linolenic acid–containing hemp seed oils, Eur. J. Lipid Sci. Technol. 122 (2020), https://doi.org/10.1002/ejlt.201900445.
[43] C. Da Porto, D. Decorti, F. Tubaro, Fatty acid composition and oxidation stability of hemp (Cannabis sativa L.) seed oil extracted by supercritical carbon dioxide, Ind. Crops Prod. 36 (2012) 401–404, https://doi.org/10.1016/j.indcrop.2011.09.015.
[44] F.L. Garcia, S. Ma, A. Dave, A. Acevedo-Fani, Structural and physicochemical characteristics of oil bodies from hemp seeds (cannabis sativa L.), Foods 10 (2021) 2930, https://doi.org/10.3390/foods10122930.
[45] M. Vecka, B. Staňková, S. Kutová, P. Tomášová, E. Tvrzická, A. Žák, Comprehensive sterol and fatty acid analysis in nineteen nuts, seeds, and kernel, SN Appl. Sci. 1 (2019) 1531, https://doi.org/10.1007/s42452-019-1576-z.
[46] T. Bögl, F. Mlynek, M. Himmelsbach, W. Buchberger, Comparison of one-phase and two-phase extraction methods for porcine tissue lipidomics applying a fast and reliable tentative annotation workflow, Talanta 236 (2022) 122849, https://doi.org/10.1016/j.talanta.2021.122849.
[47] C. Kehelpannala, T.W.T. Rupasinghe, T. Hennessy, D. Bradley, B. Ebert, U. Roessner, A comprehensive comparison of four methods for extracting lipids from Arabidopsis tissues, Plant Methods 16 (2020) 155, https://doi.org/10.1186/s13007-020-00697-z.
[48] M. Höring, C. Stieglmeier, K. Schnabel, T. Hallmark, K. Ekroos, R. Burkhardt, G. Liebisch, Benchmarking one-phase lipid extractions for plasma lipidomics, Anal. Chem. 94 (2022) 12292–12296, https://doi.org/10.1021/acs.analchem.2c02117.
[49] C.Z. Ulmer, C.M. Jones, R.A. Yost, T.J. Garrett, J.A. Bowden, Optimization of Folch, Bligh-Dyer, and Matyash sample-to-extraction solvent ratios for human plasma-based lipidomics studies, Anal. Chim. Acta 1037 (2018) 351–357, https://doi.org/10.1016/j.aca.2018.08.004.
[50] A.L. Souza, G.J. Patti, A Protocol for Untargeted Metabolomic Analysis: from Sample Preparation to Data Processing, 2021, pp. 357–382, https://doi.org/10.1007/978-1-0716-1266-8_27.
[51] A. Cerrato, S.E. Aita, A.L. Capriotti, C. Cavaliere, C.M. Montone, S. Piovesana, A. Laganà, Fully automatized detection of phosphocholine-containing lipids through an isotopically labeled buffer modification workflow, Anal. Chem. 93 (2021) 15042–15048, https://doi.org/10.1021/acs.analchem.1c02944.
[52] M. Bianco, C.D. Calvano, G. Ventura, G. Bianco, I. Losito, T.R.I. Cataldi, Regiochemical assignment of N -acylphosphatidylethanolamines (NAPE) by liquid chromatography/electrospray ionization with multistage mass spectrometry and its application to extracts of lupin seeds, J. Am. Soc. Mass Spectrom. 31 (2020) 1994–2005, https://doi.org/10.1021/jasms.0c00267.
[53] G. Ventura, C.D. Calvano, M. Bianco, A. Castellaneta, I. Losito, T.R.I. Cataldi, Pe, Or not PE, that is the question: the case of overlooked lyso- N -acylphosphatidylethanolamines, Rapid Commun. Mass Spectrom. 37 (2023), https://doi.org/10.1002/rcm.9527.
[54] A. Castellaneta, I. Losito, V. Losacco, B. Leoni, P. Santamaria, C.D. Calvano, T.R. I. Cataldi, HILIC-ESI-MS analysis of phosphatidic acid methyl esters artificially generated during lipid extraction from microgreen crops, J. Mass Spectrom. 56 (2021), https://doi.org/10.1002/jms.4784.
[55] M. Tura, M. Mandrioli, E. Valli, R.C. Rubino, D. Parentela, T. Gallina Toschi, Changes in the composition of a cold-pressed hemp seed oil during three months of storage, J. Food Compos. Anal. 106 (2022) 104270, https://doi.org/10.1016/j.jfca.2021.104270.
[56] J. Nogales-Bueno, B. Baca-Bocanegra, J.M. Hernández-Hierro, R. Garcia, J. M. Barroso, F.J. Heredia, A.E. Rato, Assessment of total fat and fatty acids in walnuts using near-infrared hyperspectral imaging, Front. Plant Sci. 12 (2021), https://doi.org/10.3389/fpls.2021.729880.
[57] L. Mondello, P.Q. Tranchida, P. Dugo, G. Dugo, Rapid, micro-scale preparation and very fast gas chromatographic separation of cod liver oil fatty acid methyl esters, J. Pharm. Biomed. Anal. 41 (2006) 1566–1570, https://doi.org/10.1016/j.jpba.2006.01.027.
[58] P. Avato, M.A. Pesante, F.P. Fanizzi, C. Aimbiré de Moraes Santos, Seed oil composition of Paullinia cupana var, sorbilis (Mart.) Ducke, Lipids 38 (2003) 773–780, https://doi.org/10.1007/s11745-003-1126-5.
[59] A.H. Banskota, A. Jones, J.P.M. Hui, R. Stefanova, I.W. Burton, Analysis of polar lipids in hemp (cannabis sativa L.) by-products by ultra-high performance liquid chromatography and high-resolution mass spectrometry, Molecules 27 (2022) 5856, https://doi.org/10.3390/molecules27185856.
[60] M. Tura, M. Mandrioli, E. Valli, T. Gallina Toschi, Quality indexes and composition of 13 commercial hemp seed oils, J. Food Compos. Anal. 117 (2023) 105112, https://doi.org/10.1016/j.jfca.2022.105112.
[61] C. Occhiuto, G. Aliberto, M. Ingegneri, D. Trombetta, C. Circosta, A. Smeriglio, Comparative evaluation of the nutrients, phytochemicals, and antioxidant activity of two hempseed oils and their byproducts after cold pressing, Molecules 27 (2022) 3431, https://doi.org/10.3390/molecules27113431.
[62] M. Irakli, E. Tsaliki, A. Kalivas, F. Kleisiaris, E. Sarrou, C.M. Cook, Effect of genotype and growing year on the nutritional, phytochemical, and antioxidant properties of industrial hemp (cannabis sativa L.) seeds, Antioxidants 8 (2019) 491, https://doi.org/10.3390/antiox8100491.
[63] K. Tsuboi, T. Uyama, Y. Okamoto, N. Ueda, Endocannabinoids and related N-acylethanolamines: biological activities and metabolism, Inflamm. Regen. 38 (2018) 28, https://doi.org/10.1186/s41232-018-0086-5.
[64] B. Wang, P. Tontonoz, Phospholipid remodeling in physiology and disease, Annu. Rev. Physiol. 81 (2019) 165–188, https://doi.org/10.1146/annurev-physiol-020518-114444.